



# Compact multiplex PCR device for HIV-1 and HIV-2 viral load determination from finger-prick whole blood in resource-limited settings

Tianyi Liu<sup>a</sup>, Anthony J. Politza<sup>b</sup>, Md Ahsan Ahamed<sup>a</sup>, Aneesh Kshirsagar<sup>a</sup>, Yusheng Zhu<sup>c</sup>, Weihua Guan<sup>a,b,\*</sup>

<sup>a</sup> Department of Electrical Engineering, Pennsylvania State University, University Park, 16802, USA

<sup>b</sup> Department of Biomedical Engineering, Pennsylvania State University, University Park, 16802, USA

<sup>c</sup> Department of Pathology and Laboratory Medicine, Pennsylvania State University, Hershey, 17033, USA



## ARTICLE INFO

### Keywords:

Human immunodeficiency viruses  
Viral load  
Self-testing  
Nucleic acid testing  
Reverse transcription polymerase chain reaction  
Quantification

## ABSTRACT

The human immunodeficiency virus (HIV) remains a major global health concern for which accurate viral load monitoring is essential for the management of HIV infection. The advent of antiretroviral therapy (ART) has transformed once-fatal HIV disease into a manageable chronic condition that now makes the need for VL testing which aims to satisfy international suppression targets 95-95-95 all the more essential. Therefore, considering the complexity and diversity of HIV infection, it is essential to develop rapid diagnostic technologies suitable for different clinical situations. Here, we report on a multiplexed PCR device developed for simple and efficient quantification of HIV-1 or HIV-2 viral loads using finger-pricked whole blood from rural decentralized settings. This device is comprised of a previously developed RNA extraction module combined with an optimized real-time PCR amplification system. Together, these combine to simultaneously detect and differentiate HIV-1 & 2; as well as adopting a testing control of RNase P allowing for full diagnostic analysis from one sample. Our device also includes an intuitive user interface and is completely autonomous so it can serve individuals in remote areas who are unfamiliar with the field of medical testing. They get the results in a very short time of around 70 min and hence save on testing times without leaving accuracy behind. The efficiency and effectiveness of the device were validated through the analysis of 30 clinical samples, yielding a sensitivity of 100% for both HIV-1 and HIV-2. The specificity was found to be 100% for HIV-1 and 90.91% for HIV-2, demonstrating high diagnostic accuracy. One of the most attractive things about this device is that it comes in comparison to all other counterparts. Given that you can run the assay for less than \$10, it could be an economically viable way to use this as a broadscale test in regions where healthcare budgets don't allow others. Hence it is quite a useful device to aid HIV management in resource-limited settings, where conventional laboratory facilities are out of reach due its simplicity and affordability with rapid output. The point-of-care test is an effective, low-cost, high quality diagnostic tool-promoting rapid testing for HIV-inexpensively overcoming the barriers to efficient control of and care in resource-limited settings.

## 1. Introduction

The Human Immunodeficiency Virus (HIV) remains an important public health issue worldwide with population-level effects that generate considerable social and economic burden (WHO, 2023, 2022). While the outcome of HIV infection is also greatly serious, an entirely different problem has arisen following the introduction and evolution of antiretroviral therapy (ART) in managing adults with HIV. However, what was once a death sentence, HIV is now a treatable chronic infection

if the proper treatment protocols are followed (Deeks et al., 2021). The success of ART is largely dependent on the accurate and frequent monitoring of viral load (VL) levels in order to assess the efficacy of treatment and stop the progression towards AIDS (Reeves et al., 2023). The international community aims to reach the 95-95-95 goals by setting ambitious global health targets based upon the year 2025 (Djyou et al., 2023). Realizing these goals relies on regular, high-quality VL testing that is essential for both the patient-level care of HIV and population-wide measures to control its spread (Mancuso et al., 2020;

\* Corresponding author. Department of Electrical Engineering, Pennsylvania State University, University Park, 16802, USA.

E-mail address: [wzg111@psu.edu](mailto:wzg111@psu.edu) (W. Guan).

Prakash et al., 2024).

HIV has added complexities due to multiple subtypes, with HIV-1 nearly exclusively in western countries where it is primarily found and a significant portion of Africa and Southeast Asia, including geographical hotspots as considered middle-lower-income (Akakpo et al., 2023). These differences in prevalence and clinical behavior necessitate a versatile approach to antiretroviral therapy (ART) monitoring, adapted to the distinct treatment needs and resistance profiles of each subtype (Pham et al., 2017). A previous study has shown that aggressive treatment strategies are crucial for patients infected with the rapid progressive HIV-1 (The Strategies for Management of Antiretroviral Therapy Study Group, 2008). HIV-2, which progresses very slowly and is often resistant to drugs that would be effective against HIV-1 (such as the non-nucleoside reverse transcriptase inhibitors NNRTIs), on the other hand requires different treatments (Charpentier et al., 2013). This difference highlights the need for flexible ART regimens aimed to appropriately treat disease based on subtype-specific features (Moranguinho et al., 2023). Moreover, dual infection with HIV-1 and HIV-2 adds to the complexity of this field rendering accurate diagnosis and treatment essential (Tchounga et al., 2023). This is a condition that warrants the application of diagnostics technology for virus type which can detect and quantify both types at once (Diop-Ndiaye et al., 2024). Critical to ensuring treatments are matched appropriately for the viral subtype, maximizing patient outcomes and contributing to global public health initiatives in management and control of the HIV epidemic (Mariani et al., 2020).

In developed nations, access to VL testing is generally straightforward due to robust healthcare infrastructure and frequent healthcare visits (Pham et al., 2022). Facilities often feature both traditional central laboratory setups and commercial point-of-care (POC) devices, such as the PIMA device, which facilitate rapid and accessible testing (Dorward et al., 2022). Technologies like the GeneXpert HIV-1 Viral Load Test and Roche's Cobas Liat™ System utilize plasma samples in controlled laboratory settings, catering primarily to developed markets with options extending to healthcare facilities and home-based self-testing (Bwana et al., 2019; Jagodzinski et al., 2019). Ongoing research and development efforts focus on enhancing these technologies in accuracy, accessibility, and speed (Ahamed et al., 2025, 2024; Ahamed and Guan, 2024; Choi et al., 2018, 2016; Curtis et al., 2016; Damhorst et al., 2015; Liu et al., 2011, 2023, 2022a, 2022b; Mauk et al., 2017; Nouri et al., 2023, 2021; Phillips et al., 2018; Politza et al., 2024, 2023; Safavieh et al., 2016; Z. Tang et al., 2022; Ahamed et al., 2024b). Despite these developments, their use is largely limited to developed areas, mainly because of challenges in processing whole blood samples and the lack of quantitative features in a single operation (Choi and Guan, 2022a, 2022b; Liao et al., 2016; Liu et al., 2022a; Phillips et al., 2019; Z. F. Tang et al., 2022). These urgent concerns underscore the essential need for creating a sophisticated HIV viral load monitoring device that functions from sample to result and is appropriate for point-of-care use.

However, in low- and middle-income countries (LMICs) there are a number of additional challenges which must be addressed for effective viral load (VL) testing beyond infrastructure-related barriers such as lack of reliable electricity (Lecher et al., 2016). A first problem is the scarcity of skilled clinicians by knowledgeable to handle the complex laboratory instrumentation necessary for VL tests, which curtails testing capabilities (Newman and Hardie, 2021). Price is also a significant hurdle. Tackling the high costs of involuntary testing infrastructure in LMICs implies that foreign aid represents a substantial contraction, as these technologies are not maintained locally and require expensive investment (Thomas et al., 2021). Furthermore, problems managing the supply chain (i.e. access to necessary materials) are made more severe by a lack of pre-existing infrastructure and result in delays around key supplies and results (Kilmarx and Simbi, 2016). Additionally, sophisticated VL testing technologies developed for settings with stable infrastructure are oftentimes ill-equipped to handle the challenging and fluctuating field conditions that prevail in many LMICs (i.e. extreme

temperatures or high humidity), which can interfere with sensitive equipment functionality (Drain et al., 2019). In LMICs, these factors highlight the dire need for more appropriate VL testing solutions and a demand for innovations that are cost-effective and environmentally stable enough to be efficiently deployed in local settings. This leaves a balkanized landscape for affordable, accessible and feasible VL testing solutions in these regions so that there is an urgent need of innovative HIV management technology.

Addressing this gap, our research introduces a novel multiplex PCR-based detection system tailored for LMICs. This battery-operated device is ideal for areas with unreliable electricity and is designed for self-testing by laypersons, eliminating the need for professional medical personnel. It is cost-effective, requiring only about \$4 per test. The device also includes a control test for accuracy and uses a four-channel detection system to differentiate between HIV-1 and HIV-2, accurately measuring viral load to monitor disease progression and adjust treatment plans. The device boasts an RNA extraction efficiency of 80% through a compact sample preparation unit, designed to collect and examine viral RNA accurately. Its semi-automated nature allows for the processing of multiple samples simultaneously, enhancing throughput and minimizing human error, thereby ensuring consistent results. Our system not only measures HIV-1 and HIV-2 viral loads simultaneously with a 96% accuracy rate but also demonstrates over HIV.

100% for HIV-1, 100% for HIV-2 sensitivity and 100% for HIV-1 and 90.91% for HIV-2 specificity in assays. These performance metrics confirm the device's capability to reliably detect HIV-1 as well as HIV-2 at various stages of infection, providing an essential tool in closing the significant gap in VL testing solutions for LMICs. This advancement is particularly vital as regular and precise VL testing is indispensable for effective global HIV control and prevention, with the added capability to manage co-infections of HIV-1 and HIV-2, underscoring its importance in the evolution of HIV management technologies.

## 2. Materials and methods

### 2.1. Materials and chemicals

Materials for this study were procured from various suppliers. RNA extraction kits, specifically the QIAamp Viral RNA Mini Kit, catalog number 52904, were sourced as detailed in *Supplementary Table S6*. Electronic and optical components for the HIV analyzer were purchased from DigiKey, as listed in *Supplementary Table S7*. RT-qPCR primers and probes were supplied by IDT, while essential reagents and chemicals were acquired from Sigma-Aldrich and Thermo Fisher Scientific. The Bio-Rad CFX96 system was employed for assay validation. Viral RNAs for HIV-1, HIV-2, and RNase P, with catalog numbers VR-3245SD, VR-3266SD, and 1006626 respectively, were obtained from ATCC. Clinical HIV samples were provided by the Penn State Hershey Medical Center. All materials were used as received and stored according to the manufacturers' guidelines.

### 2.2. Gel electrophoresis

To perform electrophoresis on dsDNA fragments, we first prepare 1x TAE buffer by diluting 100 ml of 50x TAE buffer with 4900 ml of deionized water. Next, 5 g of agarose powder is added to 100 ml of 1x TAE buffer, stirred for 30 s, and heated in a microwave for about 2 min, stirring every 30 s until dissolved. After adding 5  $\mu$ l of SYBR Safe DNA gel stain, the gel mixture is cooled for 1–2 min, poured into a mold, and left to solidify for 40 min before removing the comb. For the DNA sample and ladder preparation, we mix loading buffer with the DNA sample at a 1:5 ratio and prepare a 9.6  $\mu$ l ladder mix (1.6  $\mu$ l ladder, 1.6  $\mu$ l loading dye, and 6.4  $\mu$ l nuclease-free water). The solidified agarose gel is placed in the electrophoresis tank, filled with 1x TAE buffer, and bubbles are removed. We load 8  $\mu$ l of the ladder mix into the first well and 15  $\mu$ l of DNA samples into subsequent wells, using a sharp pipette tip for uniform

loading. The voltage is set to 110 V, and the gel runs for 45–55 min. Finally, the gel is imaged using the SYBR Safe gel application.

### 2.3. Statistical analysis

For this study, all statistical analyses and regression modeling were executed utilizing MATLAB R2020 software (Natick, MA). Data visualization, including all figures and plots, was also primarily performed with MATLAB, supplemented by Microsoft PowerPoint for layout adjustments and final presentations. Each plot displayed in the results represents the average value (mean) accompanied by three standard deviations. These measurements were consistently derived from three separate tests (triplicates) to ensure reliability unless otherwise indicated. This standard approach was maintained across all experimental conditions to facilitate accurate comparison and reproducibility of the data. The use of MATLAB was integral not only for the initial data processing but also for the subsequent analysis stages, ensuring a seamless workflow from data collection to visualization.

## 3. Results and discussion

### 3.1. Overall workflow

**Fig. 1a** illustrates the complete workflow of our multiplex viral load testing PCR-Based approach for detecting HIV-1 and HIV-2 viral loads. **Fig. 1b** details all necessary materials required for the workflow. The steps are as follows: Step 1 - Activation of the application on an Android

smartphone with step-by-step instructions. Step 2 - The user collects around 100  $\mu$ L of blood using a disposable pipette through a finger prick. Blood is collected and processed using a plasma separation card apparatus (Liu et al., 2023). The separation of plasma on filter paper as the blood passes through the card. In the datasheet for Vivid™ Plasma Separation GR, a wait time of 1 min is indicated to achieve full filtration. After separation from the rest of the whole blood specimen, plasma is ready for diagnostic or research use. Step 3 - Transfer the absorbent paper with plasma to a collection tube. The RNA are then purified using a centrifuge-based portable RNA extraction device that we previously developed (Politza et al., 2024; Zhang et al., 2024). The collected RNA is then added into a test tube that contains RT-qPCR reagents. The portability and user-friendliness of this on-site sample preparation solution, that can be done in under 10 min without the need for carrier RNA or cold storage highlights how versatile & practical the device is, especially in resource-limited settings. Step 4 - At this point, the test tube is inserted into the machine and placed in front of a device to start testing. Step 5 - The application shows the end results after 70 min. All of this can be done at home by the user, without requiring professional staff or laboratory facilities. Our system can simultaneously test samples from four patient groups to improve detection efficiency. This capacity would allow simultaneous testing for HIV viral load from multiple samples in low- and middle-income countries (LMICs).

Detailed mechanistic steps for the reaction mechanism used in this study are outlined pictorially in **Fig. 1c**. The process begins by using a custom plasma separation card that separates the red blood cells so as to isolate virus particles i.e., HIV-1, HIV-2 and RNase P in the sample.

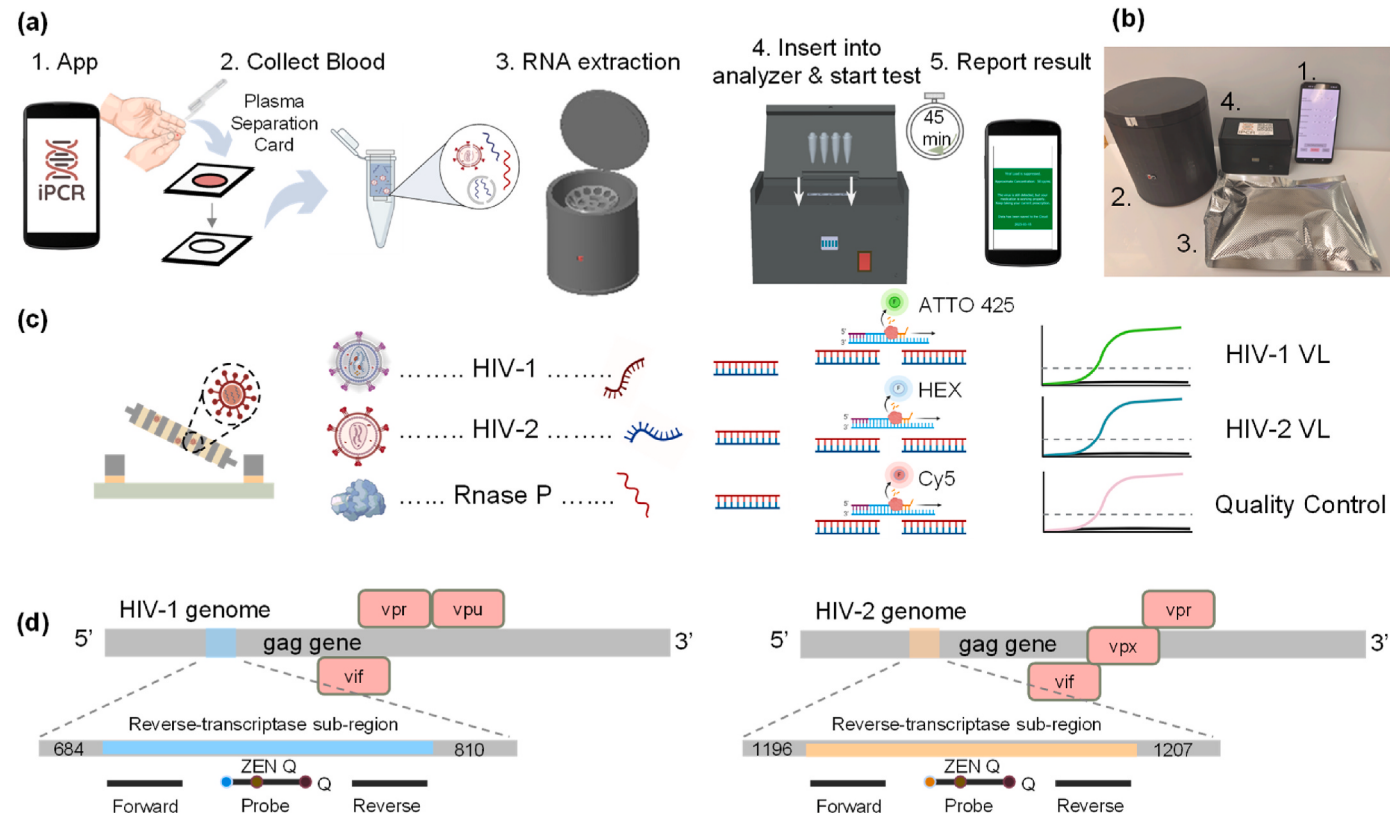


**Fig. 1.** Overall Device Workflow and Assay Design. **(a)** Outline of the procedure as detailed in the mobile application: the user starts the app, collects a blood sample using a disposable pipette and a plasma separation card, places the card into a centrifuge-based portable RNA extraction device for RNA extraction, inputs the extracted RNA with water into the test tube, and receives results via the app after 40 min. **(b)** Depiction of the device components, including: 1. An Android smartphone, 2. A centrifuge-based portable RNA extraction device, 3. Reagents and materials for testing, 4. A portable PCR analyzer. **(c)** Schematic illustrating the reaction mechanism: Step one involves separating plasma and red blood cells using a plasma separation card, which contains viruses (HIV-1, HIV-2, and RNase P). Step two extracts the viral RNA using the centrifuge-based portable RNA extraction device. Step three amplifies the RNA through portable PCR, generating a fluorescent signal. The final step determines the test results based on the fluorescent signal and cycle number. **(d)** Primer design for HIV-1 and HIV-2, featuring two RT-qPCR primers and one probe for each virus targeting the beginning of the gag gene.

Following this, Step 2 continues by isolating the viral-imparted RNA with a portable centrifuge-based reagent that streamlines rapid and efficient preparation of the extracted RNA for analysis. The third step of the mechanism is for this extracted RNA to be amplified by a useable, mobile PCR device expressing a fluorescence signal in the presence of viral RNA. In this step we use the state of art multiplex RT-qPCR technology which involves a reverse transcriptase enzyme to convert RNA into complementary DNA(cDNA) first. This cDNA is then subjected to TaqMan PCR detection, an extremely specific and sensitive technique that uses a double-labeled probe system for amplification. The multiplex RT-qPCR assay detected simultaneously with differentiating and relayed results for HIV: ATTO425, HEX and Cy5 channels targeted HIV-1, HIV-2, RNase P, respectively. Each probe has been engineered with high specificity for one of three targets, providing qPCR detection by unique fluorescent labeling (Tombuloglu et al., 2021). Such multiplex detection capabilities are essential for the robust surveillance and precise diagnosis of viruses (Guiraud et al., 2023). Interpretation of the test results is the final step in analysis, with whether or not a sample tested positive determined from fluorescent signals and how many PCR cycles were needed to reach significant levels. The advantage of this is for quantitative analysis with high level of specificity to accurately detect viral load in the sample which can be helpful in determining whether a patient is still infected or drug treatment was successfully applied.

### 3.2. Multiplex PCR assay performance

Specific primer-probe sets were designed for each target in the multiplexed assay, which includes HIV-1, HIV-2, and human RNase P. This assay also employs two reverse transcription PCR (RT-PCR) primers and one fluorescent probe per viral type, targeting the first part of gag gene (Fig. 1d). Both the Reverse-transcriptase sub-region targeting HIV-1 and its corresponding region for targeting HIV-2 are depicted in Supplementary Tables S1–2. This region was chosen because it is well conserved among various strains mnemonic, making short for better detection per wear (Curtis et al., 2012; Gaebler et al., 2021). RNase P was used as an internal control to confirm RNA extraction and general assay effectiveness, for which a unique set of primers along with a probe

were designed (Broughton et al., 2020). For detecting samples with each primer and probe set, amplification reaction mixtures were prepared that contained all combinations of primers/probes at the same concentration under a common thermal cycling protocol. We sought a strategy by which we could detect only the desired RNA targets, and limit signal for any target to their respective optical channel as much in order not need separate runs. This specificity is likely to be important in limiting cross-reactivity between the targets and ultimately improving diagnosis using our approach. Benefits of this multiplex method are increased efficiency and require less time and costs for HIV infection diagnosis. Primer and probe design were conducted with 6 primers and 3 probes, respectively for the PCR (Supplementary Tables S3, S4, and S5).

Specificity of our multiplex RT-qPCR assay is an essential parameter, directly related to the accuracy at which we can detect. It was critical that our assay had a clean and distinct signal for differentiation of HIV-1, HIV-2, and RNase P with little to no cross reactivity between them in order as an effective diagnostic tool. To determine the specificity and multiplexing ability of our assay, we performed a well-thought-out set of experiments. We systematically created eight experimental biotin samples by arranging the three targets—HIV-1, HIV-2, and RNase P—in all possible combinations, simulating a three-bit binary pattern. Each sample contained synthetic RNA sequences of these three targets and was classified as either positive or negative for each respective marker based on the presence or absence of these RNA sequences. The RNA concentrations were set at either 0 or 1000 copies per reaction, serving as a serial dilution to assess the assay's sensitivity and specificity. This design allowed for a quantitative visual analysis of each sample (Fig. 2a).

PCR amplification was performed on the samples (followed by agarose gel electrophoresis analysis as presented in Fig. 2b: after running through a final total of 60 cycles, clear-visible bands at different base pair lengths indicated presence of amplified genetic material at desired length ranges for all analyzed cases. Lanes 2, 3 and 5 in particular showed single bands corresponding to individual target amplifications (HIV-1, HIV-2 and RNase P respectively) By contrast, lanes 4, lane 6 and lane 7 showed dual bands reflecting co-amplification of two different targets per sample. Lane 8 was of particular interest because it

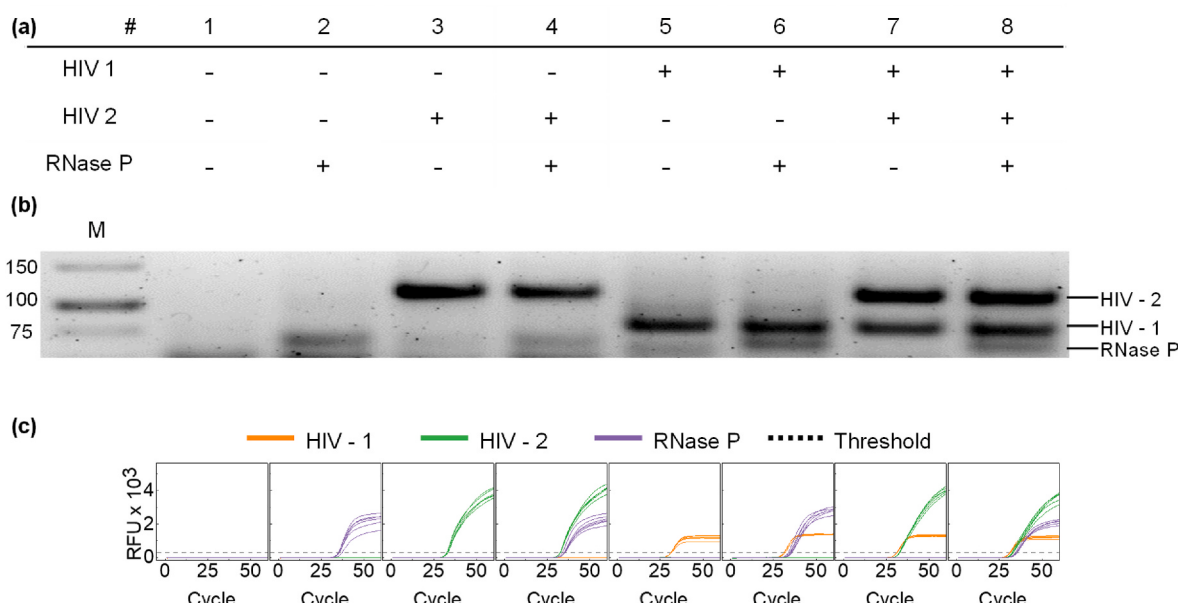


**Fig. 2.** Validation of the specificity of the multiplex RT-qPCR assay. (a) Samples 1 through 8 were created by mixing synthetic RNA of HIV-1, HIV-2, and RNase P, each positive or negative marked with “+/-” sign. The concentration of each viral RNA in the samples ranged from 0 or 1000 copies per reaction. (b) Agarose gel electrophoresis was used to analyze the RT-qPCR products, displaying the amplification profiles for Samples 1 to 8. Each sample was tested six times. (c) Results from real-time multiplex RT-qPCR amplification obtained from Bio-Rad bench top PCR analyzer for Samples 1 to 8 are presented. Optical signals for HIV-1, HIV-2, and RNase P from three different optical channels are combined into a single figure.

displayed multiple bands specific to all three targets resulting from efficient multiplex amplification, validating the ability and sensitivity of our assay for detecting more than one pathogen. No amplification was observed for NTC in lane 1, confirming the absence of contamination and non-specific amplifications. To validate the gel electrophoresis data, we quantitated selected samples to qPCR for 60 cycles. [Supplementary Fig. S8](#) Shows the full image, covering the marker (molecular weight standard), sample banding, and the start and end of electrophoresis. Fluorescence detection results, where [Fig. 2c](#) shows fluorescence and all experimental samples show a signal above the background threshold representing successful RNA amplification in target selection. This cross-validation not only confirms the accuracy of the gel electrophoresis data but also demonstrates the reliability of the assay under dynamic conditions. Since our PCR primer probe design is based on previously published, well-established designs, we did not further test for false positives with non-HIV pathogens. Taken together, our results from both basic and advanced analyses strongly indicated that the PCR assay is highly specific with high multiplexing capability, rendering it ideal as a candidate for external integration into portable diagnostic platforms

developed against rapid diagnosis of infectious diseases in point-of-care testing formats. This simplification of this assay is a major step forward in molecular diagnostics especially when simultaneous comprehensive detection for multiple viral targets uses to be performed at resource-limited settings.

### 3.3. Analyzer development and sub-module validation

Next, we developed a portable analyzer prototype ( $170 \times 118 \times 74$  mm) capable of multiplex RT-qPCR amplification and fluorescent signal quantification. [Fig. 3a](#) presents the disassembled views of the device. This portable unit is loaded with an internal lithium-ion battery and Bluetooth wireless technology, bringing together electronic, optical and thermal cycling components at the small lab scale. [Supplementary Fig. S1](#) illustrates the graphical user interface (GUI) for the mobile phone. [Supplementary Fig. S2](#) illustrates a simple block diagram of the entire device as well as a complete flowchart explaining about developing an android GUI. Commercial products of a similar type, such as the 'm-PIMA HIV-1/2 VL cartridge,' cost approximately \$27 per test,

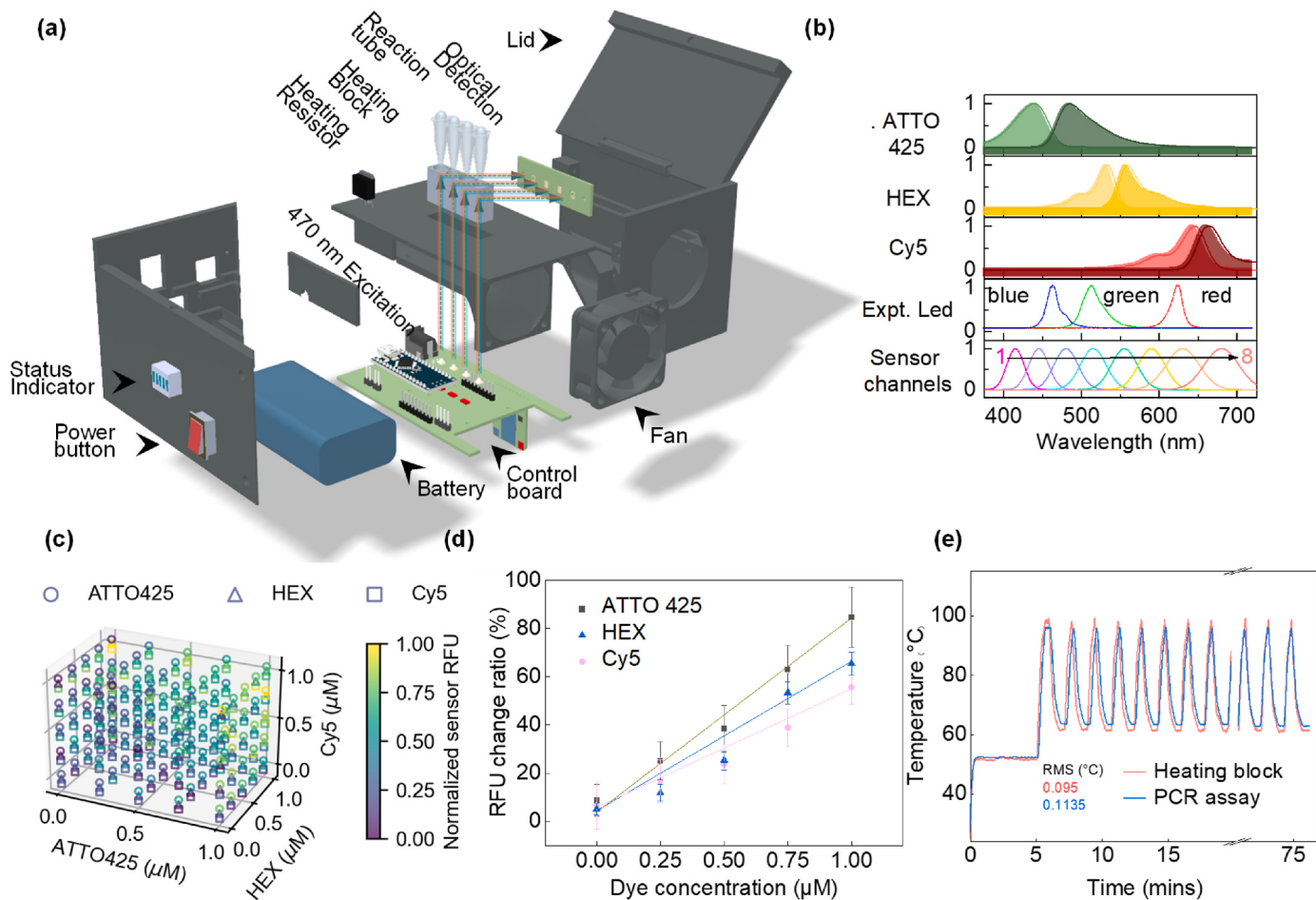


**Fig. 3.** The probable PCR analyzer design and its sub module validation. **(a)** Illustrations depict a fully enclosed analyzer and a partial exploded view. The unit features Bluetooth connectivity for wireless data transmission and incorporates integrated optical and thermal cycling subsystems for efficient nucleic acid analysis. It operates on an internal rechargeable battery. **(b)** Presented are the theoretical excitation and emission spectra for three selected fluorophores—ATTO425, HEX, and Cy5—alongside the RGB excitation sources and the sensor's eight distinct detection channels. The blue, green, and red light sources are optimally matched with the excitation spectra of ATTO425, HEX, and Cy5, respectively, while the detection channels 4, 6, and 8 correspond closely with their emission spectra. **(c)** A 3D scatter plot shows normalized sensor RFU responses to varying concentrations of mixed fluorophores. The plot uses the optimal excitation sources and detection channels noted in (a), with 125 unique combinations of ATTO425, HEX, and Cy5 tested at five concentrations (0, 0.25, 0.5, 0.75, and 1  $\mu\text{M}$ ). The visualization highlights the increasing RFU trends correlated with rising fluorophore concentrations, independent of the levels of the other two fluorophores. **(d)** Evaluation of the optical sensor's response to different fluorophores. Each sensor channel demonstrated a linear response across fluorophore concentrations ranging from 0 to 1  $\mu\text{M}$ . Measurements were conducted using a 256X gain, a 154 ms integration time, and 80% PWM for the RGB LED excitation control. **(e)** Temperature profile for the PCR assay's heating block, detailing the stages of heating, incubation, and cooling throughout the PCR cycle.

whereas our device requires only about \$4 per test (Diop-Ndiaye et al., 2024). More detailed information on the materials and fabrication processes of the each type of analyzer can be seen in [Supplementary Table S7](#). It orients the devices perpendicularly and employs custom-designed circuit boards for heat control & fluorescence. Task results can also be viewed via a custom GUI on mobile phone supporting Bluetooth. PCB Circuit Design can be found on [Supplementary Fig. S3](#). The Arduino and Android code are available in the supplementary materials.

We have updated our analyzer, based on the NAT-On-USB device (Liu et al., 2022a) and HIVL device (Liu et al., 2023), by incorporating an optical module with four unique excitation and detection units for real-time fluorescence tracking. Our optical system, aimed at analyzing mixtures of fluorophores, employs an RGB LED (SK6812) for excitation and a CMOS spectral sensor (AS7341) as the detector. These components are arranged perpendicularly to minimize excitation interference. Since there are no optical paths at the top of the reaction tube, a hot lid function is not needed to mitigate vapor interference with detection. The LED combines three light sources, managed by an Arduino Nano, while the sensor functions across eight visible spectrum channels, modifying integration times and using I<sub>2</sub>C protocol for communication. The sensor incorporates monolithic filters with nano-optic technology on its CMOS, capturing light with a photodiode array and converting it into digital signals through a 16-bit ADC, as illustrated in [Fig. 3b](#). Our emission sensor features eight channels, theoretically supporting multiplex detection of up to eight targets. In contrast, current technologies, such as Biomeme, can support a maximum of only three ([Franklin® Real-Time PCR Thermocycler, nd](#)). This configuration allows for the sequential activation of LEDs to monitor emissions across four channels concurrently, removing the need for additional optical elements and simplifying the detection of fluorophores without hardware alterations. Due to the different excitation light sources and sensor channels used for the three targets in this optical system, comparisons can only be made within individual channel fluorescence intensity changes. We explored the impact of one fluorophore's presence on the detectability of others within a mixed scenario. For this purpose, we created a sample set containing five concentrations (0.00, 0.25, 0.50, 0.75, and 1.00  $\mu\text{M}$ ) for each fluorophore, leading to 125 distinct combinations. These combinations, along with the normalized RFUs for each fluorophore's optimal channels, are showcased in [Fig. 3c](#). An upward trend in RFUs is noticeable as fluorophore concentrations increase. For more precise analysis, we plotted the RFUs against the concentration for each fluorophore, ignoring the concentrations of the others, to present the data clearly in a two-dimensional format. Our data processing method involves zeroing the baseline before calculating the Ct value based on the threshold. This approach may lead to the erroneous assignment of Ct values to S-shaped curves, highlighting the need for improved data processing algorithms in the future, such as incorporating machine learning methods. [Fig. 3d](#) demonstrates strong linearity for ATTO425, HEX, and Cy5, indicating that this detection method is suitable for precise sub-micromolar measurements of these fluorophores, which can be used for our multiplex RT-qPCR assay.

In developing our portable PCR analyzer, achieving precise temperature control and rapid heating and cooling is crucial. We engineered a temperature control module featuring an aluminum heating block with a hollow design to reduce mass and enhance the speed of temperature changes. A 2  $\Omega$  power resistor heats the block swiftly, while a fan, paired with ducting and a heat sink, cools it efficiently. The schematic of the thermal module is shown in [Supplementary Figs. S4a and S4b](#). Both fan and resistor are controlled via a PID temperature function on an Arduino Nano, powered by a 9V source. We used Type K/T thermocouples with a National Instrument deck to measure temperatures. One set was on the heating block surface, and another was in the reaction solution. [Fig. 3e](#) displays the temperature fluctuations throughout the test cycle, monitoring both the block and the fluid temperatures in the PCR assay. Completing the cycle, including reverse

transcription, initial denaturation, denaturing, annealing/extending, and 40 cycles, takes about 70 min. Our thermal cycling module achieves a maximum heating rate of 1.82 °C/s and a cooling rate of 1.31 °C/s, approximately 15 min slower than a Bio-Rad benchtop PCR (Nguyen et al., 2022). The RMS for the heating block and PCR assay fluid temperatures are 0.095 and 0.1135, respectively. Increasing the ramp rate to further accelerate the reaction speed is one of the key directions for future research. [Supplementary Fig. S4c](#) illustrates the power profile over a 77-min test cycle, with a peak power of approximately 30W. The entire test consumes 14.2 Wh of energy, and it can be powered by a 20 Wh EBL rechargeable lithium battery ([Supplementary Fig. S4d](#)). A full charge supports only one complete testing cycle. Despite being slower than the Bio-Rad benchtop PCR, our device's simple structure, compact size, and battery operability meet the temperature standards required for PCR reactions, making it valuable in resource-limited settings, particularly in LMICs (Mogg and Bond, 2003).

### 3.4. Analyzer analytical evaluation

In order to evaluate the performance of our assay in identifying viral presence over a wide range of clinical and field scenarios, we carried out an extended sensitivity comparison versus standard benchtop PCR utilizing multiplexed HIV-1, HIV-2 detection with RNase P on portable analyzer. The initial phase involved assessing the assay's aptitude to quantify precise RNA levels across a wide range of concentrations, from 1 to  $10^5$  copies/rnx. As illustrated in [Fig. 4a](#), real-time multiplex RT-qPCR trials were conducted on a Bio-Rad desktop PCR analyzer with serial dilutions of synthetic RNA standards, spanning from  $10^5$  to 0 copies/rnx, each replicated six times across three independent optical channels. Due to sample availability, we were unable to conduct additional repetitions at this time. However, we will consider this in future studies. This benchmark utilized the Bio-Rad instrument to establish the detection thresholds for each virus, found to be 5 copies/ $\mu\text{L}$  for both HIV-1, HIV-2, and the RNase P reference gene. Additionally, the calculated amplification efficiencies are as follows: HIV-1 at 103.37%, HIV-2 at 99.67%, and RNase P at 106.9%. This addition provides a more comprehensive explanation. The precision of these conclusions was corroborated by additional analyses. These insights are detailed expansively in [Fig. 4b](#), exhibiting the highly quantitative capabilities of our approach.

To additionally validate the absolute quantification of our portable analyzer systematically, we performed validation measurements across a RT-qPCR array panel from various serially diluted RNA samples ([Fig. 4c](#)). All concentrations of RNA were performed in triplicate to demonstrate reproducibility (from  $10^5$  to 0 copies/rnx). Comparative analysis between our portable device and traditional Bio-Rad analyzer demonstrated the amplification curves generated by testing each of RNA type with two systems were identical. The HEX channel in the self-developed instrument exhibited reduced reaction efficiency and insufficient amplification, particularly at higher concentration ranges, due to suboptimal primer design and lower temperature control precision, resulting in nonlinear characteristics. Comparing the results ([Fig. 4d](#)) gave a correlation coefficient of between 0.96 and 0.99. Meanwhile, the combination of a portable PCR analyzer with a multiplex RT-qPCR assay can achieve a detection limit of up to 10 copies per reaction. Although this is not as low as the 5 copies per reaction achieved with conventional PCR equipment, it is sufficient for HIV VL testing. These results are evidence of the validity and applicability of our portable PCR with respect to conventional laboratory devices. These results highlight the utility of this analyzer for viral loads in quantitative analysis. Collectively, these findings underscore the superior performance of our multiplex assay when deployed on our portable analyzer, confirming its suitability for use in a variety of settings, including those with limited resources. The assay's ability to deliver sensitive, specific, and reliable results in a portable format presents significant advantages for on-site diagnostics and real-time monitoring of viral loads. This makes our

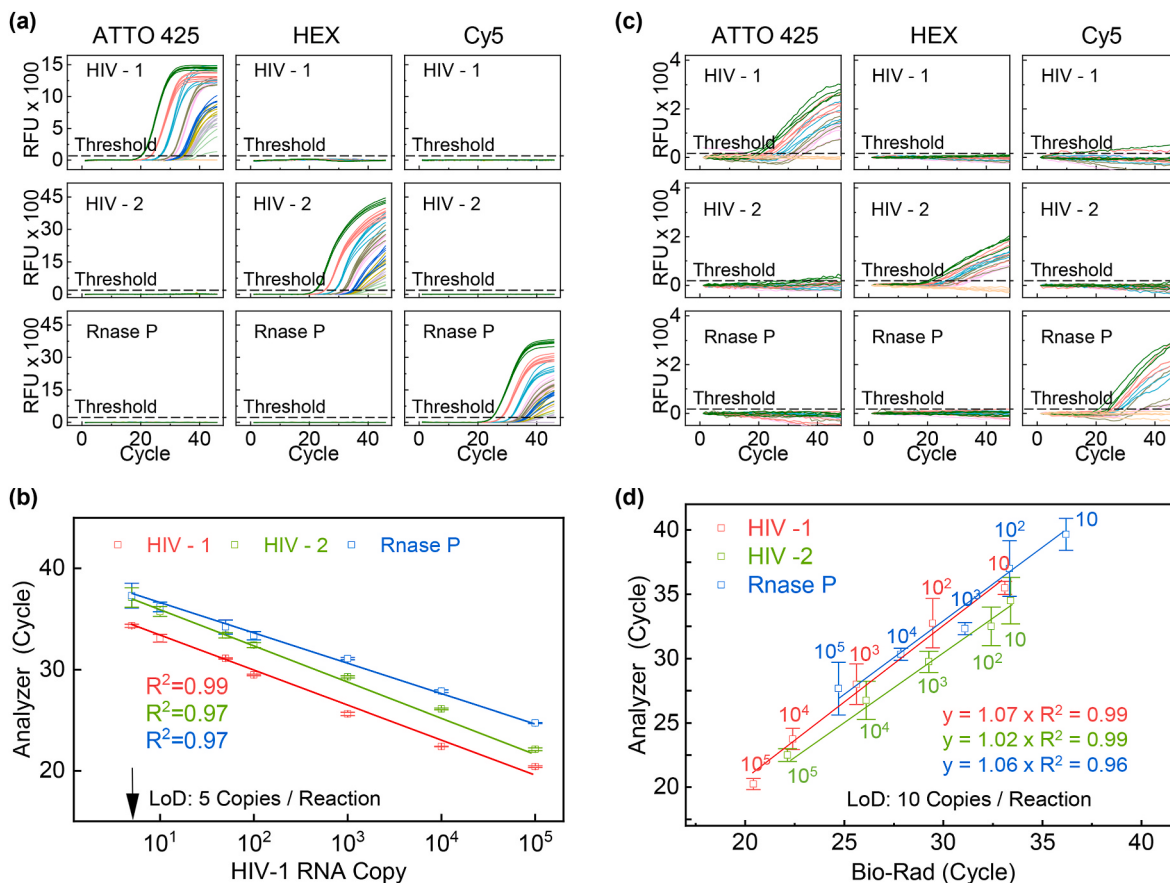


**Fig. 4.** Evaluation of Sensitivity and Quantitative Performance of Multiplex RT-qPCR Assays Using Bio-Rad Equipment and a Portable PCR Analyzer. (a) This figure illustrates the results from real-time multiplex RT-qPCR using a Bio-Rad benchtop PCR analyzer with serially diluted RNA standards at concentrations ranging from 10<sup>5</sup> to 0 copies per reaction, replicated six times. Optical detection for HIV-1, HIV-2, and RNase P across three distinct optical channels is shown in three separate columns. (b) The graph displays the cycle threshold (Ct) values at varying RNA concentrations for each target. The "Cq values" is marked by the duration required for relative fluorescence units (RFU) to exceed a threshold of 20 (indicated by a dashed line in the plot). (c) A panel displaying RT-qPCR data from tests on serially diluted RNA, with HIV concentrations from 10<sup>5</sup> to 0 copies per reaction, each tested in triplicate. Optical signals for the three targets are again split into three columns. (d) A comparative plot shows the Ct values obtained with both the Bio-Rad benchtop PCR analyzer and our portable analyzer for all three targets.

portable analyzer a crucial tool in the global effort to control and manage HIV, especially in regions where access to traditional lab facilities is constrained.

### 3.5. Diagnostic performance from sample to answer

To show the clinical utility of our HIV VL PCR instrument, we subjected a total of 30 archived samples that have been extracted from HIV positive symptomatic subscribers who had already enrolled into one or two programs within Penn State Hershey Medical Center's infectious diseases and consultative services. Multimodal plasma samples of 13 positive HIV-1/2 individuals at various viral load (VL) levels. 17 healthy blood donors were identified as confirmed HIV-1 and HIV-2 negative by Roche COBAS® AmpliPrep. Given the lack of clinical samples from HIV-2-infected patients, we spiked extracted RNA with synthetic HIV-2 RNA to simulate the conditions of such infections within our study. It is important to note that all positive clinical samples contained only HIV-1, and HIV-2 was entirely negative.

We compared our HIV VL PCR device with a conventional benchtop RT-qPCR by testing two identical samples with both methods to evaluate consistency. Further, traditional centrifugation methods were employed for RNA extraction, followed by RT-qPCR testing on these samples to assess our device's performance agreement with the benchtop RT-qPCR. Each analysis utilized an identical volume of 25  $\mu$ L, though the benchtop RT-qPCR employed a column-based extraction method. Each clinical sample was tested just once. One set of data comes from the traditional

extraction method and amplified by a conventional qPCR instrument, while the other set comes from using our portable extraction module and PCR analyzer. Fig. S5 displays the RT-qPCR results of these clinical samples alongside six concentration references for quantification. This figure also includes a calibration curve, illustrating the robustness of our testing approach. Fig. S6 display the optical signals obtained from 30 clinical samples processed through our portable centrifuge RNA extraction module, as detected in the HIV VL PCR device. The signals for HIV-1, HIV-2, and RNase P, derived from three distinct optical channels, are consolidated into a unified figure. Additionally, Fig. S7 features RT-qPCR analysis results from our HIV VL PCR device for a cohort of 30 clinical samples, encompassing both positive and negative outcomes. Fig. 5a presents a detailed qualitative and quantitative analysis of HIV-1, HIV-2, and RNase P results from both the benchtop RT-qPCR and our device. White boxes highlight samples from uninfected individuals or those successfully undergoing antiretroviral therapy (ART) with a fully suppressed viral load within the safe threshold (Low: 0–1000). Light red or green boxes denote samples with viral loads exceeding safe limits, indicating a need for enhanced medical oversight(Medium: 1000–20,000). Dark red or blue boxes reveal a significantly higher viral load, signaling potential treatment failure and a risk of viral rebound despite ongoing ART(High: >20,000 copies/mL) (Ritchie et al., 2014; Saag et al., 1996). A heatmap on the right side of the figure provides reference values to further guide interpretation.

Fig. 5b, which serves as a table, summarizes the Diagnostic Performance of our device. We carefully compared the Cq values from our

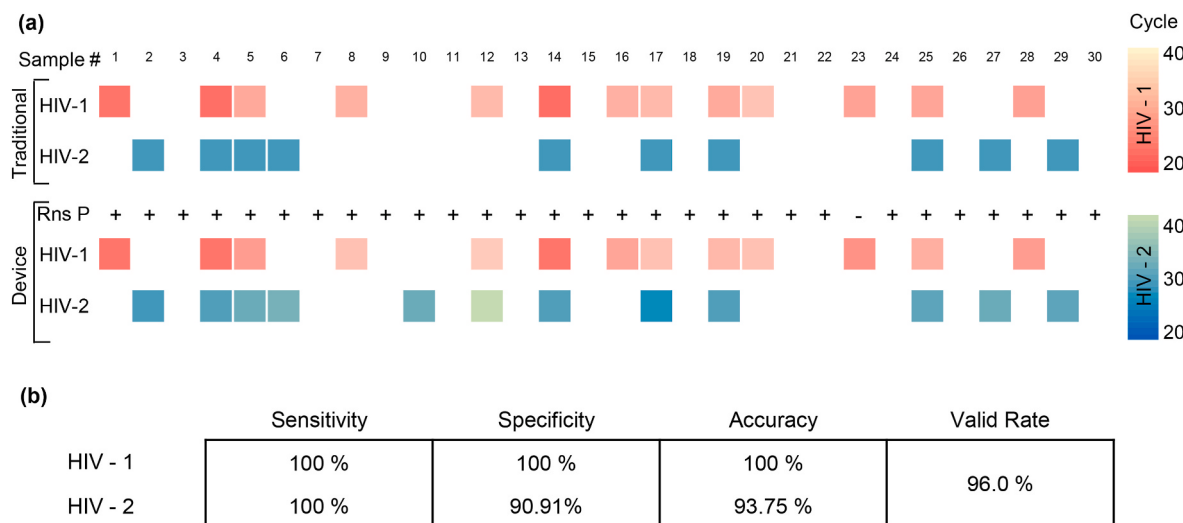


**Fig. 5.** Evaluation of Clinical Samples with Our Device. **(a)** Validation with Constructed Clinical Samples in a Blind Test. RNA from HIV-1 and RNase P was extracted from the plasma of 30 patients utilizing our centrifuge-based portable RNA extraction device. After sample preparation, HIV-2 RNA was introduced to the extracted RNA. Qualitative analysis for RNase P and quantitative analyses for HIV-1 and HIV-2 were performed using our device and a Bio-Rad benchtop PCR system. A heat map displays the Ct values from the quantitative analyses of HIV-1 and HIV-2. **(b)** Diagnostic Performance Overview: This table displays the performance metrics of our system, including Sensitivity, Specificity, Accuracy and Valid Rate for HIV-1, HIV-2, and RNase P.

device with those from the benchtop PCR to evaluate our analyzer's capabilities in quantitative viral load analysis. Our device incorporates a quality control method to eliminate invalid tests, achieving a high testing validity rate of 96%. For HIV-1 and HIV-2, the sensitivity was 100% and 100%, specificity was 100% and 90.91%, and accuracy was 100% and 93.75% respectively, confirming that our device performs on par with traditional laboratory protocols using benchtop RT-PCR. These findings robustly support the implementation of our innovative point-of-care platform in settings where precise and reliable HIV viral load testing is essential.

#### 4. Conclusion

In conclusion, our research introduces a pioneering multiplex PCR-based device specifically engineered for effective HIV-1 and HIV-2 viral load testing in resource-limited settings. This portable and battery-operated system overcomes significant logistical and technical challenges by offering high levels of sensitivity and specificity, essential for managing HIV effectively. Demonstrating a sensitivity of 100% for both HIV-1 and HIV-2, and a specificity of 100% for HIV-1 and 90.91% for HIV-2, our device sets a new benchmark in the field of HIV diagnostics. Furthermore, the device successfully achieved a diagnostic accuracy of 100% for HIV-1 and 93.75% for HIV-2, confirming its reliability and effectiveness in a range of testing environments. The entire testing process can be completed in approximately 60 min, offering a significant time advantage over traditional lab-based tests. Moreover, the cost per test has been reduced to under \$10, making it financially accessible for widespread deployment in low-resource settings. These performance metrics and cost-efficiency are critical for enhancing access to vital health metrics, supporting ongoing treatment efforts, and aligning with global health initiatives like the 95-95-95 targets set by the World Health Organization. The device's ability to deliver rapid, robust, and accurate viral load results directly at the point-of-care marks a substantial advancement in HIV management, particularly in low-resource settings where traditional testing facilities are not readily accessible. The device may still encounter challenges such as sample contamination and result interpretation. To address these, we will integrating automated sample processing, utilizing disposable consumables, and employing machine learning for standardized results in the future development. Extensive testing and comprehensive user training

are essential for ensuring stability and reliability. The potential of this technology to transform HIV diagnostics and treatment in these regions is immense, underscoring the vital role of innovative diagnostic solutions in combating the global HIV/AIDS epidemic.

#### CRediT authorship contribution statement

**Tianyi Liu:** Writing – review & editing, Writing – original draft, Visualization, Validation, Supervision, Software, Project administration, Methodology, Investigation, Formal analysis, Data curation, Conceptualization. **Anthony J. Politza:** Writing – original draft, Validation, Software, Methodology, Formal analysis, Data curation. **Md Ahasan Ahamed:** Writing – review & editing, Writing – original draft, Data curation. **Aneesh Kshirsagar:** Writing – review & editing, Writing – original draft, Data curation. **Yusheng Zhu:** Resources. **Weihua Guan:** Writing – review & editing, Writing – original draft, Visualization, Project administration, Funding acquisition, Conceptualization.

#### Declaration of generative AI in scientific writing

During the preparation of this work, the authors used ChatGPT (powered by OpenAI's language model, GPT-4; <http://openai.com>) in order to refine the manuscript text for grammatical correctness and to improve readability. After using this tool/service, the author(s) reviewed and edited the content as needed and take full responsibility for the content of the publication.

#### Declaration of competing interest

A provisional patent application has been submitted concerning the technology discussed in this document.

#### Acknowledgment

The research conducted was funded by the National Institutes of Health (R33AI147419, R33HD105610) and the National Science Foundation (1912410 and 1902503, 2319913). Any opinions, findings, conclusions, or recommendations detailed in this publication are those of the authors alone and do not necessarily reflect the official views of the National Science Foundation or the National Institutes of Health.

## Supplementary information

The Supplementary information to this article can be found online.

## Appendix A. Supplementary data

Supplementary data to this article can be found online at <https://doi.org/10.1016/j.bios.2024.116997>.

## Data availability

Data will be made available on request.

## References

- Ahamed, M.A., Guan, W., 2024. *Biophys. J.* 123, 145a.
- Ahamed, M.A., Politza, A.J., Liu, T., Khalid, M.A.U., Zhang, H., Guan, W., 2024. *Nanotechnology* 36, 042001.
- Ahamed, M.dA., Khalid, M.A.U., Dong, M., Politza, A.J., Zhang, Z., Kshirsagar, A., Liu, T., Guan, W., 2024b. *Biosens. Bioelectron.* 246, 115866.
- Akakpo, P.K., Ken-Amoah, S., Enyan, N.I.E., Agyare, E., Salia, E., Baidoo, I., Derkyi-Kwarteng, L., Asare, M., Adjei, G., Addo, S.A., Obiri-Yeboah, D., 2023. *Infect. Agents Cancer* 18, 33.
- Broughton, J.P., Deng, X., Yu, G., Fasching, C.L., Servellita, V., Singh, J., Miao, X., Streithorst, J.A., Granados, A., Sotomayor-Gonzalez, A., Zorn, K., Gopez, A., Hsu, E., Gu, W., Miller, S., Pan, C.-Y., Guevara, H., Wadford, D.A., Chen, J.S., Chiu, C.Y., 2020. *Nat. Biotechnol.* 38, 870–874.
- Bwana, P., Ageng'o, J., Mwau, M., 2019. *PLoS One* 14, e0213865.
- Charpentier, C., Camacho, R., Ruelle, J., Kaiser, R., Eberle, J., Gürtler, L., Pironi, A., Stürmer, M., Brun-Vézinet, F., Descamps, D., Obermeier, M., 2013. *Clin. Infect. Dis.* 56, 1654–1658.
- Choi, G., Guan, W., 2022a. Sample-to-Answer microfluidic nucleic acid testing (NAT) on lab-on-a-disc for malaria detection at point of need. In: Ossandon, M.R., Baker, H., Rasooly, A. (Eds.), *Biomedical Engineering Technologies, Methods in Molecular Biology*. Springer US, New York, NY, pp. 297–313.
- Choi, G., Guan, W., 2022b. An ultracompatract real-time fluorescence loop-mediated isothermal amplification (LAMP) analyzer. In: Ossandon, M.R., Baker, H., Rasooly, A. (Eds.), *Biomedical Engineering Technologies, Methods in Molecular Biology*. Springer US, New York, NY, pp. 257–278.
- Choi, G., Prince, T., Miao, J., Cui, L., Guan, W., 2018. *Biosens. Bioelectron.* 115, 83–90.
- Choi, G., Song, D., Shrestha, S., Miao, J., Cui, L., Guan, W., 2016. *Lab Chip* 16, 4341–4349.
- Curtis, K.A., Rudolph, D.L., Morrison, D., Guelig, D., Diesburg, S., McAdams, D., Burton, R.A., LaBarre, P., Owen, M., 2016. *J. Virol. Methods* 237, 132–137.
- Curtis, K.A., Rudolph, D.L., Nejad, I., Singleton, J., Beddoe, A., Weigl, B., LaBarre, P., Owen, S.M., 2012. *PLoS One* 7, e31432.
- Damhorst, G.L., Duarte-Guevara, C., Chen, W., Ghonge, T., Cunningham, B.T., Bashir, R., 2015. *Engineering* 1, 324–335.
- Deeks, S.G., Archin, N., Cannon, P., Collins, S., Jones, R.B., De Jong, M.A.W.P., Lambotte, O., Lamplough, R., Nduing'u, T., Sugarman, J., Tiemessen, C.T., Vandekerckhove, L., Lewin, S.R., The International AIDS Society (IAS) Global Scientific Strategy working group, Core Leadership Group, Deeks, S., Lewin, S., De Jong, M., Working Group 1 (Understanding HIV reservoirs), Ndhllovu, Z., Chomont, N., Brumme, Z., Deng, K., Jasenosky, L., Jefferys, R., Orta-Resendiz, A., Working Group 2 (HIV reservoir measurement), Mardarelli, F., Nijhuis, M., Bar, K., Howell, B., Schneider, A., Turk, G., Nabatanzi, R., Working Group 3 (Mechanisms of virus control), Blankson, J., Garcia, J.V., Paillardini, M., Lunzen, J.V., Antoniadi, C., Cortes, F.H., Working Group 4 (Targeting the provirus), Valente, S., Søgaard, O.S., Diaz, R.S., Ott, M., Dunham, R., Schwarze, S., Patrigeon, S.P., Nabukenya, J., Working Group 5 (Targeting the immune system), Caskey, M., Mothe, B., Wang, F.S., Fidler, S., SenGupta, D., Dressler, S., Matoga, M., Working Group 6 (Cell and gene therapy), Kiem, H.-P., Tebas, P., Kityo, C., Dropulic, B., Louella, M., Das, K.T., Working Group 7 (Paediatric remission and cure), Persaud, D., Chahroudi, A., Luzuriaga, K., Puthanakit, T., Safrit, J., Masheto, G., Working Group 8: (Social, behavioral and ethical aspects of cure), Dubé, K., Power, J., Salzwedel, J., Likhitwonnawut, U., Taylor, J., Nuh, O.L., Dong, K., Kankaka, E.N., 2021. *Nat. Med.* 27, 2085–2098.
- Diop-Ndiaye, H., Sène, P.Y., Coulibaly, K., Diallo, M., Diallo, S., Diop, K., Sow-Ndoye, A., Fall, M., Ndiaye, A.J.S., Mathebula, E., Ba, A.A., Lejeune, C., Manga, N.M.P., Camara, M., Ndour, C.T., Kane, C.T., 2024. *J. Virol. Methods* 324, 114872.
- Djiyou, A.B.D., Penda, C.I., Madec, Y., Ngondi, G.D., Moukoko, A., Varloteaux, M., De Monteynard, L.-A., Moins, C., Moukoko, C.E.E., Aghokeng, A.F., 2023. *BMC Pediatr.* 23, 119.
- Dorward, J., Naidoo, J., Moodley, P., Sookrajh, Y., Samsunder, N., Sayed, F., Naicker, N., Fanshawe, T., Drain, P.K., Lessells, R.J., Hayward, G., Butler, C.C., Garrett, N., 2022. *JAIDS Journal of Acquired Immune Deficiency Syndromes* 91, 189–196.
- Drain, P.K., Dorward, J., Bender, A., Lillis, L., Marinucci, F., Sacks, J., Bershteyn, A., Boyle, D.S., Posner, J.D., Garrett, N., 2019. *Clin. Microbiol. Rev.* 32, e00097, 18.
- Franklin® Real-Time PCR Thermocycler [WWW Document], n.d. . Biomeme, Inc. URL <https://shop.biome.com/franklin-real-time-pcr-thermocycler/> (accessed 8.3.24).
- Gaebler, C., Falcinelli, S.D., Stoffel, E., Read, J., Murtagh, R., Oliveira, T.Y., Ramos, V., Lorenzi, J.C.C., Kirchherr, J., James, K.S., Allard, B., Baker, C., Kuruc, J.D., Caskey, M., Archin, N.M., Siliciano, R.F., Margolis, D.M., Nussenweig, M.C., 2021. *J. Virol.* 95, e01986, 20.
- Guiraud, V., Bocobza, J., Desmonet, M., Diamond, F., Plantier, J.-C., Moreau, G., Wirde, M., Stefic, K., Barin, F., Gautheret-Dejean, A., 2023. *J. Clin. Microbiol.* e00619–23.
- Jagodzinski, L.L., Manak, M.M., Hack, H.R., Liu, Y., Malia, J.A., Freeman, J., Phanuphak, N., De Souza, M., Kroon, E.D., Colby, D.J., Chomchey, N., Lally, M.A., Michael, N.L., Ananworanich, J., Peel, S.A., 2019. *J. Clin. Microbiol.* 57, e01922, 18.
- Kilmarx, P.H., Simbi, R., 2016. *PLoS Med.* 13, e1002089.
- Lecher, S., Williams, J., Fonjungo, P.N., Kim, A.A., Ellenberger, D., Zhang, G., Toure, C., Agolory, S., Appiah-Pippin, G., Beard, S., Borget, M.Y., Carmona, S., Chipungu, G., Diallo, K., Downer, M., Edgil, D., Haberman, H., Hurlston, M., Jadzak, S., Kiyaga, C., MacLeod, W., Makumb, B., Mutai, H., Mwangi, C., Mwangi, J. W., Mwasekaga, M., Naluguza, M., Ng'Ang'A, L.W., Nguyen, S., Sawadogo, S., Sleeman, K., Stevens, W., Kuritsky, J., Hader, S., Nkengasong, J., 2016. *MMWR Morb. Mortal. Wkly. Rep.* 65, 1332–1335.
- Liao, S.C., Peng, J., Mauk, M.G., Awasthi, S., Song, J., Friedman, H., Bau, H.H., Liu, C., 2016. *Sensor. Actuator. B Chem.* 229, 232–238.
- Liu, C., Geva, E., Mauk, M., Qiu, X., Abrams, W.R., Malamud, D., Curtis, K., Owen, S.M., Bau, H.H., 2011. *The Analyst* 136, 2069–2076.
- Liu, T., Choi, G., Tang, Z., Kshirsagar, A., Politza, A.J., Guan, W., 2022a. Fingerpick blood-based nucleic acid testing on a USB interfaced device towards HIV self-testing. *Biosens. Bioelectron.*
- Liu, T., Choi, G., Tang, Z., Kshirsagar, A., Politza, A.J., Guan, W., 2022b. *Biosens. Bioelectron.* 209, 114255.
- Liu, T., Politza, A.J., Kshirsagar, A., Zhu, Y., Guan, W., 2023. *ACS Sens. acssensors.3c01819.*
- Mancuso, P., Chen, C., Kaminski, R., Gordon, J., Liao, S., Robinson, J.A., Smith, M.D., Liu, H., Sariyer, I.K., Sariyer, R., Peterson, T.A., Donadoni, M., Williams, J.B., Siddiqui, S., Bunnell, B.A., Ling, B., MacLean, A.G., Burdo, T.H., Khalili, K., 2020. *Nat. Commun.* 11, 6065.
- Mariani, D., De Azevedo, M.C.V.M., Vasconcellos, I., Ribeiro, L., Alves, C., Ferreira, O.C., Tanuri, A., 2020. *J. Clin. Virol.* 122, 104212.
- Mauk, M., Song, J., Bau, H.H., Gross, R., Bushman, F.D., Collman, R.G., Liu, C., 2017. *Lab Chip* 17, 382–394.
- Mogg, R.J., Bond, J.M., 2003. *Mol. Ecol. Notes* 3, 666–668.
- Moranguinho, I., Taveira, N., Bartolo, I., 2023. *Indian J. Manag. Sci.* 24, 5905.
- Newman, H., Hardie, D., 2021. *Rev. Med. Virol.* 31, e2165.
- Nguyen, P.Q.M., Wang, M., Ann Maria, N., Li, A.Y., Tan, H.Y., Xiong, G.M., Tan, M.-K.M., Bhagat, A.A.S., Ong, C.W.M., Lim, C.T., 2022. *Microsyst Nanoeng* 8, 82.
- Nouri, R., Jiang, Y., Politza, A.J., Liu, T., Greene, W.H., Zhu, Y., Nunez, J.J., Lian, X., Guan, W., 2023. *ACS Nano* 17, 10701–10712.
- Nouri, R., Tang, Z., Dong, M., Liu, T., Kshirsagar, A., Guan, W., 2021. *Biosens. Bioelectron.* 178, 113012.
- Pham, M.D., Nguyen, H.V., Anderson, D., Crowe, S., Luchters, S., 2022. *BMC Publ. Health* 22, 1203.
- Pham, M.D., Romero, L., Parnell, B., Anderson, D.A., Crowe, S.M., Luchters, S., 2017. *AIDS Res. Ther.* 14 (3).
- Phillips, E.A., Moehling, T.J., Bhadra, S., Ellington, A.D., Linnes, J.C., 2018. *Anal. Chem.* 90, 6580–6586.
- Phillips, E.A., Moehling, T.J., Ejendal, K.F.K., Hoilett, O.S., Byers, K.M., Basing, L.A., Jankowski, L.A., Bennett, J.B., Lin, L.K., Stanciu, L.A., Linnes, J.C., 2019. *Lab Chip* 19, 3375–3386.
- Politza, A.J., Liu, T., Guan, W., 2023. *Lab Chip* 23, 3882–3892.
- Politza, A.J., Liu, T., Kshirsagar, A., Dong, M., Ahamed, M.dA., Guan, W., 2024. A Portable Centrifuge for Universal Nucleic Acid Extraction at the Point-of-Care.
- Prakash, S., Asarey, R., Priyatma, Sharma, M., Khan, S., Medha, 2024. *Sci. Rep.* 14, 8700.
- Reeves, D.B., Gaebler, C., Oliveira, T.Y., Peluso, M.J., Schiffer, J.T., Cohn, L.B., Deeks, S.G., Nussenweig, M.C., 2023. *Nat. Commun.* 14, 4186.
- Ritchie, A.V., Ushiro-Lumb, I., Edemaga, D., Joshi, H.A., De Ruiter, A., Szumilin, E., Jendruik, I., McGuire, M., Goel, N., Sharma, P.I., Allain, J.-P., Lee, H.H., 2014. *J. Clin. Microbiol.* 52, 3377–3383.
- Saag, M.S., Holodniy, M., Kuritzkes, D.R., O'Brien, W.A., Coombs, R., Poscher, M.E., Jacobsen, D.M., Shaw, G.M., Richman, D.D., Volberding, P.A., 1996. *Nat. Med.* 2, 625–629.
- Safavieh, M., Kanakasabapathy, M.K., Tarlan, F., Ahmed, M.U., Zourob, M., Asghar, W., Shafee, H., 2016. *Acs biomater. Sci Eng* 2, 278–294.
- Tang, Z., Cui, J., Kshirsagar, A., Liu, T., Yon, M., Kuchipudi, S.V., Guan, W., 2022. *ACS Sens.* 7, 2370–2378.
- Tang, Z.F., Cui, J.R., Kshirsagar, A., Liu, T.Y., Yon, M., Kuchipudi, S.V., Guan, W.H., 2022. *ACS Sensors.*
- Tchounga, B.K., Bertine, M., Diamond, F., Ferré, V.M., Inwoley, A., Boni, S.P., Moisan, A., Plantier, J.-C., Descamps, D., Ekouevi, D.K., Charpentier, C., 2023. *PLoS One* 18, e0283602.
- The Strategies for Management of Antiretroviral Therapy (SMART) Study Group, 2008. *J infect dis.* 197, 1133–1144.
- Thomas, R., Probert, W.J.M., Sauter, R., Mwenge, L., Singh, S., Kanema, S., Vanqa, N., Harper, A., Burger, R., Cori, A., Pickles, M., Bell-Mandla, N., Yang, B., Bwalya, J., Phiri, M., Shanaube, K., Floyd, S., Donnell, D., Bock, P., Ayles, H., Fidler, S., Hayes, R.J., Fraser, C., Hauck, K., 2021. *Lancet Global Health* 9, e668–e680.
- Tombuloglu, H., Sabit, H., Al-Suhaimi, E., Al Jindan, R., Alkharsah, K.R., 2021. *PLoS One* 16, e0250942.

WHO, 2022. HIV Key Facts.

WHO, 2023. Summary of the global HIV epidemic. <https://www.who.int/data/gho/d ata/themes/hiv-aids>.

Zhang, Z., Liu, T., Dong, M., Ahamed, MdA., Guan, W., 2024. WIREs Nanomed Nanobiotechnol 16, e1969.